A benzodiazepine ligand with improved GABA$_A$ receptor α5-subunit-selectivity driven by interactions with loop C

Xenia Simeone*, Filip Koniuszewski, Markus Müllegger, Andreas Smetka, Friederike Steudle, Roshan Puthenkalam, Margot Ernst[$], Petra Scholze[$]

[$]Corresponding authors: margot.ernst@meduniwien.ac.at; petra.scholze@meduniwien.ac.at

Center for Brain Research, Medical University of Vienna, Vienna, Austria

1

Running title: A new α5-selective benzodiazepine ligand

Correspondence to be addressed to:

Petra Scholze

Medical University of Vienna, Austria

Center for Brain Research

Spitalgasse 4

A-1090 Vienna, Austria

tel: +43 1 40160 34092

fax: +43 1 40160 934093

ORCID-ID: 0000-0003-4984-6034

e-mail: petra.scholze@meduniwien.ac.at

Additional corresponding author:

Margot Ernst

Medical University of Vienna, Austria

Center for Brain Research

Spitalgasse 4

A-1090 Vienna, Austria

tel: +43 1 40160 34065

fax: +43 1 40160 934053

ORCID-ID: 0000-0002-9809-2649

e-mail: margot.ernst@meduniwien.ac.at

Numbers

Number of Pages: 37

Number of Figures: 6

Number of Tables: 4

Number of References: 51

Number of words in Abstract: 231 words

Number of words in Introduction: 799 words

Number of words in Discussion: 1151 words

ABBREVIATIONS

CNS, central nervous system; NAM, negative allosteric modulator; PAM, positive allosteric

modulator; TEV, two-electrode voltage clamp.

Abstract

The family of GABA$_A$ receptors is an important drug target group in the treatment of sleep disorders, anxiety, epileptic seizures and many others. The most frequent GABA$_A$ receptor subtype is composed of two α, two β and one γ2-subunit, while the nature of the α-subunit critically determines the properties of the benzodiazepine binding site of those receptors. Nearly all of the clinically relevant drugs target all GABA$_A$ receptor subtypes equally. In the past years, however, drug development research has focused on studying α5-containing GABA$_A$ receptors. Beyond the CNS, α5-containing GABA$_A$ receptors in airway smooth muscles are considered as emerging target for bronchial asthma. Here, we investigated a novel compound derived from the previously described imidazobenzodiazepine SH-053-2′F-R-CH3 (SH53d-ester). While SH53d-ester is only moderately selective for α5-subunit containing GABA$_A$ receptors, the derivative SH53d-acid shows superior (>40-fold) affinity selectivity, and is a positive modulator. Using two-electrode voltage clamp electrophysiology in *Xenopus laevis* oocytes and radioligand displacement assays with HEK 293 cells, we demonstrated that an acid group as substituent on the imidazobenzodiazepine scaffold leads to large improvements of functional and binding selectivity for α5β3γ2 over other αxβ3γ2 GABA$_A$ receptors. Atom level structural studies provide hypotheses for the improved affinity to this receptor subtype. Mutational analysis confirmed the hypotheses, indicating that loop C of the GABA$_A$ receptor α-subunit is the dominant molecular determinant of drug selectivity. Thus, we characterize a promising novel α5-subunit-selective drug candidate.

Significance statement

In the current study we present the detailed pharmacological characterization of a novel compound derived from the previously described imidazobenzodiazepine SH-053-2′F-R-CH3. We describe its superior (>40-fold) affinity selectivity for α5-containing GABA$_A$ receptors and show atom level structure predictions to provide hypotheses for the improved affinity to this receptor subtype. Mutational analysis confirmed the hypotheses, indicating that loop C of the GABA$_A$-receptor α-subunit is the dominant molecular determinant of drug selectivity.

Introduction

GABA$_A$ receptors are GABA-gated chloride channels which are expressed in neurons, glial cells and several non-neuronal cell types (Gladkevich et al., 2006; Mizuta et al., 2008; Olsen and Sieghart, 2008; Barragan et al., 2015; Wan et al., 2015) where they influence a variety of cellular processes through ligand-gated chloride flux. These receptors are pentamers of subunits that are comprised of different subunit classes. The existence of six α, three β, three γ, the δ, ε, θ, π, and three ρ subunits in mammalian systems gives rise to an enormous theoretical diversity of GABA$_A$ receptor subtypes with distinct subunit composition and unique pharmacological properties. Due to the presence of multiple GABA$_A$ receptor subunits in individual cells, however, an unequivocal identification of a receptor subtype is difficult (Olsen and Sieghart, 2008). So far, the native expression of only 11 subunit combinations has been conclusively demonstrated. In addition, there is strong evidence for the existence of several other subunit combinations, the number of which is slowly increasing (Olsen and Sieghart, 2008).

GABA$_A$ receptors in the central nervous system (CNS) are the site of action of a variety of pharmacologically and clinically important drugs such as benzodiazepines, barbiturates, anesthetics, that allosterically modulate GABA-induced currents eliciting anticonvulsant, sedative-hypnotic and anxiolytic effects (Brickley and Mody, 2012; Rudolph and Mohler, 2014; Sieghart, 2015). In addition to these synthetic drugs, a wide range of natural products (Khom et al., 2010; Lorenz et al., 2010; Hanrahan et al., 2011), as well as some endogenous agents, such as neuroactive steroids (Belelli and Lambert, 2005), the endocannabinoid 2-arachidonoyl glycerol (2-AG) (Sigel et al., 2011), histamine (Saras et al., 2008; Fleck et al., 2012) and dopamine (Hoerbelt et al., 2015) modulate GABA$_A$ receptors.

The benzodiazepine binding site is located at the extracellular α+/γ- interface of the GABA$_A$ receptors (Sigel and Luscher, 2011; Richter et al., 2012). Thus, the potency and efficacy of benzodiazepine site ligands is dependent on the subtype of both of these subunits. In the CNS, benzodiazepine ligands exert mostly anxiolytic, anticonvulsive, sedative hypnotic, and myo-relaxant properties (Sieghart, 2015; Sieghart and Savic, 2018). The individual effects of

6

benzodiazepines seem to be predominantly mediated by distinct GABA$_A$ receptor subtypes and drugs specifically interacting with these subtypes are thus expected to exhibit quite selective pharmacological and behavioral effects (Mohler, 2011).

One of the first relatively α5β3γ2-selective positive allosteric modulators reported was the imidazobenzodiazepine SH-053-2′F-R-CH3 (SH53d-ester), featuring a window of separation between the modulation of α5β3γ2 receptors and α1-, α2-, or α3β3γ2 receptors (Savic et al., 2010). In electrophysiological experiments, SH53d-ester is selective for α5 receptors at low nM concentration. At 100 nM concentration, this compound markedly enhances GABA elicited currents at α1β3γ2, α2β3γ2, α3β3γ2, and α5β3γ2 receptors (Fischer et al., 2010; Savic et al., 2010). Concomitantly, this compound has moderate affinity for the benzodiazepine binding site of α5β3γ2 receptors and low affinity for α1-, α2-, or α3β3γ2 receptors (Fischer et al., 2010).

Ester to amide substitution in SH53d-ester led to MP-III-022, with improved selectivity, efficacy, and kinetic behavior as a positive modulator of GABA$_A$ receptors containing the α5 subunit (Stamenic et al., 2016). Accordingly, binding affinities of MP-III-022 (Ki) for the different receptor subtypes α1β3γ2, α2β3γ2, α3β3γ2, and α5β3γ2 expressed in HEK 293 cells were 850, 360, 660 and 55 nM, respectively. TEVC-electrophysiology in oocytes revealed allosteric modulation of MP-III-022 in α5β3γ2 GABA$_A$ receptors with efficacies of 300% at 100 nM, while being non- (α1) or only weakly modulatory at α2- and α3-containing receptors.

Clinically applied drugs targeting GABA$_A$ receptors are mainly used for their effects on the human CNS (Sieghart, 2015). However, considerable interest in these receptors expressed in peripheral tissues as potential therapeutic targets has emerged (Gladkevich et al., 2006; Mizuta et al., 2008; Sengupta et al., 2014; Barragan et al., 2015; Gallos et al., 2015; Wan et al., 2015). Of specific interest are GABA$_A$ receptors expressed in airway smooth muscle (ASM) and their ability to induce relaxation of an established contraction which could have enormous clinical implications in bronchoconstrictive diseases such as asthma. It was shown that the α5-preferring chiral imidazobenzodiazepine SH53d-ester relaxes ASM and enhances

7

chloride currents in cultured ASM cells (Gallos et al., 2015), thus suggesting that benzodiazepine sensitive α5βγ2 containing receptors are present.

The derivative of SH53d-ester, which we characterize here (called SH53d-acid, formerly known as Compound 2), has also been tested in this assay and shown to be effective (Forkuo et al., 2017), while a detailed presentation of the compound's pharmacology was still missing. In the current study we now provide this detailed pharmacological characterization of SH53d-acid and describe its superior (>40-fold) affinity selectivity for α5-containing GABA$_A$ receptors. Computational docking provides a hypothesis for the improved affinity to this receptor subtype. Using mutational analysis, we were able to identify loop C of the GABA$_A$ receptor α-subunit as the dominant molecular determinant of drug selectivity.

Materials and Methods

Compounds

SH-053-2′F-R-CH3 = SH53d-ester: *(R)*-8-ethynyl-6-(2-fluorophenyl)-4-methyl-4*H*-benzo[*f*]imidazo[1,5-*a*][1,4]diazepine-3-carboxylic acid ethyl ester;

SH53d-acid: (*R*)-8-Ethynyl-6-(2-fluorophenyl)-4-methyl-4*H*-benzo[*f*]imidazo[1,5-*a*][1,4]diazepine-3-carboxylic acid;

Figure 1

All compounds listed above were synthesized at the Department of Chemistry and Biochemistry, University of Wisconsin—Milwaukee. For details of SH53d-acid synthesis see "compound 2" in (Forkuo et al., 2017).

[^{3}H]Flunitrazepam (specific activity 83 Ci/mmol) and [^{3}H]Ro 15-4513 (specific activity 49.5 Ci/mmol) were purchased from Perkin Elmer NEN (New England Nuclear) (Waltham, Massachusetts, USA). Diazepam (7-chloro-1,3-dihydro-1-methyl-5-phenyl-2H-1,4, benzodiazepine-2-one) from Nycomed (Opfikon, Switzerland). Standard chemicals came from Sigma-Aldrich (St. Louis, Missouri, USA).

GABA$_A$ receptor subunits and mutated subunits

cDNAs of rat GABA$_A$ receptor subunits α1, α2, α3, α5, β3 and γ2S (GenBank accession numbers: NM_183326.2, NM_001135779.2, NM_017069.3, NM_017295.1, NM_017065.1, NM_183327.1) were cloned into pCI expression vectors. The mutant subunits (for details on the nomenclature of the mutated amino acids see Supplemental Figure 1 and Supplemental Table 2) were constructed using the Q5 Site-Directed Mutagenesis Kit (New England Biolabs) following manufacturer's instruction using the primers designed with the NEBaseChanger online tool (https://nebasechanger.neb.com) and listed in Table 1. The mutated subunits were confirmed by sequencing.

Table 1

Culturing of human embryonic kidney 293 cells

Human embryonic kidney (HEK) 293 cells (American Type Culture Collection ATCC® CRL-1574[TM]) were maintained in Dulbecco's modified Eagle medium (DMEM, high glucose, GlutaMAX[TM] supplement, Gibco 61965-059, ThermoFisher, Waltham, Massachusetts, USA) supplemented with 10% fetal calf serum (Sigma-Aldrich F7524, St. Louis, Missouri, USA), 100 U/ml Penicillin-Streptomycin (Gibco 15140-122, ThermoFisher, Waltham, Massachusetts, USA) and MEM (Non-Essential Amino Acids Gibco 11140-035, ThermoFisher, Waltham, Massachusetts, USA) on 10 cm cell culture dishes (Cell[+], Sarstedt, Nürnbrecht, Germany) at 37°C and 5% CO_2.

HEK 293 cells were transfected with cDNAs encoding rat $GABA_A$ receptor subunits subcloned into pCI expression vectors. The ratio of plasmids used for transfection with the calcium phosphate precipitation method (Chen and Okayama, 1987) were 3 µg α (1, 2, 3 or 5) : 3 µg β3 : 15 µg γ2 per 10 cm dish. Medium was changed 4-6 h after transfection. Cells were harvested 72 h after transfection by scraping into phosphate buffered saline. After centrifugation (10 min, 12,000 g, 4°C) cells were resuspended in TC50 (50 mM Tris-Citrate pH=7.1), homogenized with an ULTRA-TURRAX® (IKA, Staufen, Germany) and centrifuged (20 min, 50,000 g). Membranes were washed three times in TC50 as described above and frozen at -20 °C until use.

Radioligand binding assay

Frozen HEK 293 membranes were thawed, resuspended in TC50 and incubated for 90 min at 4 °C in a total of 500 µl of a solution containing 50 mM Tris/citrate buffer, pH=7.1, 150 mM NaCl and 2 nM [³H]flunitrazepam or 5 nM [³H]Ro 15-4513 in the absence or presence of 5 µM diazepam or 50 µM Ro 15-1788 (to determine non-specific binding; final DMSO concentration 0.5%). Membranes were filtered through Whatman GF/B filters (GE Healthcare, distributed by VWR Austria) and rinsed twice with 4 ml of ice-cold 50 mM Tris/citrate buffer. Filters were transferred to scintillation vials and subjected to scintillation counting after the addition of 3 ml Rotiszint Eco plus liquid scintillation cocktail (Lactan, Graz,

10

Austria). Non-specific binding determined in the presence of 5 µM diazepam or 50 µM Ro 15-1788 was subtracted from total binding to determine specific binding.

In order to determine the equilibrium binding constant K_D for the various receptor subtypes, membranes were incubated with various concentrations of the radioligand in the absence or presence of an inhibitor. Saturation binding experiments were analyzed using the equation $Y=B_{max}*X/(K_D+X)$. Nonlinear regression analysis of the displacement curves used the equation: log(inhibitor) vs. response - variable slope $Y=100/(1+10^{((logIC_{50}-x)*Hillslope)})$ with Top=100%; Bottom=0%; and HillSlope=-1. Both analyses were performed using GraphPad Prism version 8.3.0 for Mac OS X, GraphPad Software, La Jolla, California, USA, www. graphpad.com. Drug concentrations resulting in half maximal inhibition of specific [3H]-ligand binding (IC_{50}) were converted to Ki values by using the Cheng-Prusoff relationship (Cheng and Prusoff, 1973) $Ki=IC_{50}/(1+(S/K_D))$ with S being the concentration of the radioligand (2 nM for [3H]flunitrazepam or 5 nM for [3H]Ro 15-4513) and the measured K_D values (see Table 4).

Statistical analysis

One-way ANOVA followed by Tukey's multiple comparisons test was performed using GraphPad Prism version 8.3.0 for Mac OS X, GraphPad Software, La Jolla, California, USA, www. graphpad.com. The full ANOVA analysis is shown in the supplemental data.

RNA preparation

RNA was prepared as described (Simeone et al., 2017): After linearizing the cDNA vectors with appropriate restriction endonucleases, the cDNA was purified and concentrated with the DNA Clean and ConcentratorTM Kit (Zymoresearch, Catalog No. D4005). Capped transcripts of the purified cDNA were produced using the mMESSAGE mMACHINE® T7 transcription kit (Ambion, TX, USA) and polyadenylated using the Ambion PolyA tailing kit (Ambion). After transcription and polyadenylation the RNA was purified with the MEGAclearTM Kit (Ambion, Catalog No. AM1908). The final RNA concentration was

measured on NanoDrop® ND-1000 and finally diluted and stored in diethylpyrocarbonate-treated water at −80 °C. For the microinjection, the RNA of αβγ receptor combinations was mixed at 1:1:5 for αxβ3γ2 (x = 1,2,3) and 3:1:5 for α5β3γ2. All receptor combinations had a final concentration of 56 ng/µl.

Two-electrode voltage clamp electrophysiology

Electrophysiological experiments with *Xenopus laevis* oocytes have been described previously (Simeone et al., 2017). Defolliculated cells were obtained from commercial suppliers (EcoCyte Bioscience Europe, Dortmund, Germany). Healthy oocytes were injected with an aqueous solution of mRNA. A total of 2.5 ng of mRNA per oocyte was injected with a Nanoject II (Drummond). Subunit ratio was 1:1:5 for αxβ3γ2 (x = 1,2,3) and 3:1:5 for α5β3γ2. After injection of mRNA, oocytes were incubated at 18 °C in ND96 solution (96 mM NaCl, 2 mM KCl, 1 mM $MgCl_2$, 5 mM HEPES; pH 7.5) containing penicillin G (10000 IU/100 mL) and streptomycin (10 mg/100 mL) for at least 36 h before electrophysiological recordings. For current measurements, oocytes were impaled with two microelectrodes filled with 2M KCl with 1-1.5 MΩ resistance. The oocytes were constantly washed by a flow of 6 ml/min NDE (96 mM NaCl, 2 mM KCl, 1 mM $MgCl_2$, 5 mM HEPES, $CaCl_2$x$2H_2O$ 1.8mM; pH 7.5) that could be switched to NDE containing GABA and/or drugs. Drugs were diluted into NDE from DMSO solutions resulting in a final concentration of 0.1% DMSO. The EC_{3-5} was determined at the beginning of each experiment. Maximum currents measured in mRNA injected oocytes were in the microampere range for all receptor subtypes. Compounds were co-applied with GABA until a peak response was observed. Enhancement of the chloride current was defined as $(I_{GABA+Comp}/I_{GABA})$ - 1, where $I_{GABA+Comp}$ is the current response in the presence of a given compound and I_{GABA} is the control GABA current. Between two applications, oocytes were washed in NDE for up to 15 min to ensure full recovery from desensitization. SH53d-acid did not affect the pH of the measuring buffer (7.51-7.52) over the whole concentration range of the compound. pH was measured in the buffer alone, in GABA EC3-5 and in GABA EC3-5 containing SH53d-acid at 1nM-10µM. Since the measurement buffer keeps the pH

12

constant, we can be sure that over the dose response curve the protonation state of the compound does not change. Beyond this observation, we cannot draw any conclusions about the influence of the protonation state on the activity. It seems reasonable to assume that this compound is, as organic acid, deprotonated at physiological pH. As has been discussed in Forkuo et al. 2018, this is beneficial for topical application (Forkuo et al., 2018). All recordings were performed at room temperature at a holding potential of -60 mV using a Dagan CA-1B Oocyte Clamp or a Dagan TEV-200A TEV amplifier (Dagan Corporation, Mineapolis, MN, USA). Data were digitized using a Digidata 1322A or 1550 data acquisition system (Axon Instruments, Union City, CA, USA), recorded using Clampex 10.5 software (Molecular Devices, Sunnyvale, CA, USA) and analyzed using Clampfit 10.5. Data were analyzed using GraphPad Prism v.6. and plotted as concentration-response curves. These curves were normalized and fitted by non-linear regression analysis to the equation $Y = bottom + (top-bottom)/1+10(LogEC_{50}-X)*nH$, where EC_{50} is the concentration of the compound that increases the amplitude of the GABA-evoked current by 50% and nH is the Hill coefficient. Data are given as mean ± SD from at least three oocytes of two or more oocyte batches. Statistical significance was calculated using an extra sum of squares F-Test. P-values of <0.05 were accepted as statistically significant.

Computational docking

The experimental structures 6HUO, 6D6T and 6A96, containing the α1γ2-interface, were employed for this study. The 6A96 structure does not contain a benzodiazepine site. The α5 subunit's extracellular domain (ECD) of 6A96 overlaps well with the α1 subunits in 6HUO, 6D6T and 6D6U. Thus, since benzodiazepine-bound states are of interest, we used 6HUO and 6D6T to generate homology models of the extracellular α5+/γ2- interface on the basis of the alprazolam- and flumazenil-bound experimental structures using Modeller (Sali and Blundell, 1993) for the subsequent docking. Molecular docking was performed with the program GOLD (Jones et al., 1997). The numbering of the amino acids in the figures corresponds to mature human protein UniProtKB-accession IDs P14867 for α1 and P31644

13

for α5 (for comparison between rat and human amino acid numbering see Supplemental Table 2). The putative binding site was set around the CB atom of the α5Ser209 that lies on the loop C with a cut-off distance of 12 Å. Five amino acids of the γ2 subunit and five of the α5 subunit were selected to have flexible side chains: γ2Asp56, γ2Tyr58, γ2Phe77, γ2Thr142, γ2Arg144 and α5Tyr163, α5Thr208, α5Ser209, α5Thr210, α5Tyr213 respectively. Soft potentials were chosen for α5Thr208, α5Ser209, α5Thr210 and α5Gly211 to simulate backbone flexibility of loop C. The ligand was docked with the protonated carboxylic acids group fully flexible, and the seven-ring restrained to what is seen in the experimental structures (a control run with a flexible seven-ring gave very similar results). The poses were scored with GoldScore and rescored with ChemScore, as implemented in GOLD. For each ligand and each protein the top 100 (GoldScore) poses were generated with default settings.

Results

SH53d-acid has superb affinity, efficacy, and selectivity

Since the ester to amide substitution in SH53d-ester led to MP-III-022 with improved binding and efficacy selectivity, more substituents were explored. Here, we present an acid substituted compound with superior affinity selectivity. In order to directly compare the properties of this novel compound SH53d-acid to its parent compound SH53d-ester, both were measured at identical conditions side by side in radioligand binding assays as well as in two electrode voltage clamp experiments. While SH53d-acid still displays low affinity for α1-, α2-, or α3β3γ2 receptors (in the µM range) in radioligand binding assays, the affinity towards α5β3γ2 is approximately 10fold higher than the parent compound, now being in the low nM range (see Figure 2B and Table 2). SH53d-acid has superior (>40-fold) affinity selectivity for α5- over α1-containing GABA$_A$ receptors, much more selective than MP-III-022 (15-fold) and SH53d-ester (9-fold). There is also a clear window of separation between α5- and α3-containing GABA$_A$ receptors with an affinity selectivity of 16-fold in SH53d-acid, compared to

14

12-fold in MP-II-022 while being only 7-fold in SH53d-ester. Compared to α3-containing GABA$_A$ receptors the differences in affinities are 13-fold (SH53d-acid), being nearly equal to the parent compound SH53d-ester (15-fold) while MP-III-022 has the least difference (6-fold). In two electrode voltage clamp experiments we not only observed a similar affinity shift, but also greatly enhanced efficacy in modulating GABA induced currents in α5-containing receptors compared to the other receptors analyzed (Figure 2D and Table 3). The SH53d-acid has a wider window of separation, with nearly no modulatory activity in the non-α5 subtypes up to 30 nM (see Table 3). As is also the case for diazepam, the efficacy is higher in α3-containing receptors compared to α2-containing receptors, but unlike diazepam, is highest in α5-containing receptors (Savic et al., 2010).

Figure 2

Table 2

Table 3

The acid group of SH53d-acid is predicted to be in contact with loop C

In order to provide a structural hypothesis for the extraordinary potency preference of the novel ligand SH53d-acid, we performed a computational study utilizing the recently published flumazenil- and alprazolam-bound structures PDB IDs 6D6T and 6D6U (Zhu et al., 2018) and PDB ID 6HUO (Masiulis et al., 2019), together with homology models and computational docking as established in our labs (Elgarf et al., 2018; Siebert et al., 2018).

Figure 3 shows the unligated pocket of the recently released heteropentameric cryo-EM structure PDB ID 6D6T (Phulera et al., 2018) and the α5 subunits of the PDB ID 6A96 structures (Liu et al., 2018), providing an overview of the pocket contributing amino acids of these two α isoforms. At the time of writing, no experimental structures of the other α isoforms were available.

Figure 3

Computational docking has resulted in two different binding modes as candidates for benzodiazepine and imidazobenzodiazepine based ligands, previously termed BMI and BMII (Richter et al., 2012; Middendorp et al., 2014; Elgarf et al., 2018; Siebert et al., 2018). The

15

R-substituted chiral analogues of SH53d-ester have been proposed previously to utilize BMI (Elgarf et al., 2018), which later was observed experimentally for flumazenil in the 6D6T and 6D6U structures (Zhu et al., 2018). For the triazolobenzodiazepine alprazolam on the other hand, a binding mode was observed experimentally which corresponds to BMII (Richter et al., 2012; Middendorp et al., 2014; Masiulis et al., 2019).

Both the flumazenil and the alprazolam bound structures were determined with the α1 subunit, while for α5 so far only an interface with a β subunits is available (Liu et al., 2018), see Figure 3. Since the structural similarity between these two α isoforms is sufficiently high, we took advantage of the induced fit states of the flumazenil- and alprazolam-bound states and generated the α5- containing homologues from these. Subsequent computational docking into the original α1-containing structures and the α5-containing models produced similar posing space for both isoforms. The results for the α5-containing pocket yield a diversity of highly ranked poses without a clear favorite: Docking SH53d-acid into the models of both the flumazenil bound pocket and the alprazolam bound pocket yielded among both top 20 Chemscore and Goldscore results both flumazenil-like (BMI) and alprazolam-like (BMII) poses, as well as unrelated binding modes. Similarity was assessed by computing pairwise root mean square deviation (RMSD) of the common atoms of the three ligands in the superposed pairs of experimental structure with the models. Among the solutions with RMSD 0.5 – 1.5 Å compared to alprazolam, 5 layed to the Chemscore top 20 and two were in the Goldscore top 20. In the comparison with flumazenil poses with RMSD up to 2 Å contained two in the Chemscore top 20. Thus, the alprazolam-like binding mode was observed more often, but higher level of computational methods would be needed for firm conclusions. Representative poses are depicted in Figure 4.

Figure 4

Importantly, both binding modes position the acid group in close proximity to segment (loop) C of the pocket. Thus, for both binding modes the structural evidence predicts a strong impact of diverging amino acids in segment C to drive the affinity differences, while the difference in segment (loop) B should be of less influence. In order to test this structural

16

hypothesis, we studied conversion mutants. For the mutational work, we sought to narrow down the influence of amino acids that are different among α isoforms, but do not contribute to the α5- unique properties. In segment C, the α5 and α1 subunits differ in two pocket forming amino acids (see Figure 3), while the α5 and α3 subunits differ only in one of these. We therefore chose to compare the two subunits which share more amino acids in the pocket and proceeded to the mutational analysis with a side by side comparison of the α5 and α3 subunits as described in the methods.

Choice of radioligand: 3H-Flunitrazepam proves to be unsuitable

Based on our computational analysis we decided to generate mutated subunits: In the B-loop amino acids proline and threonine were exchanged between α3 and α5, generating an α3T215P- and an α5P197T- subunit. Likewise, in the C-loop amino acids serine and threonine were switched, generating α3S257T and α5T239S. Those mutated α-subunits were co-transfected with β3γ2 in HEK 293 cells and the receptors formed analyzed via radioligand binding experiments.

Equilibrium binding assays showed that receptors composed of α5(P197T)β3γ2 bind [^{3}H]Flunitrazepam with similar high affinity as α5(wt)β3γ2 (K_D: 1.9 ± 0.2 nM and 2.2 ± 0.3 nM respectively). In contrast α5(T239S)β3γ2 receptors lost this high affinity binding and showed a tenfold shift in K_D to 23.4 ± 6.1 nM (see Figure 5).

Figure 5

Radioligand displacement studies cannot be performed using a low-affinity ligand. Therefore, α5(T239S)β3γ2 receptors could not easily have been analyzed using [^{3}H]Flunitrazepam and we needed to search for another radioligand: Casula et al (Casula et al., 2001) described similar mutants in their publication, and showed that the benzodiazepine Ro 15-4513 had a much higher affinity to the mutated receptors compared to flunitrazepam. We therefore decided to test [^{3}H]Ro 15-4513 as possible radioligand and equilibrium binding assays were performed on transfected HEK 293 cells. As shown in Table 4 [^{3}H]Ro 15-4513 exhibited high affinity binding for all constructs/receptors tested.

Table 4

Conversion mutations confirm loop B is not the determinant of the selectivity

We transfected HEK 293 cells with various GABA$_A$ receptor subunit combinations and performed radioligand displacement assays with 5 nM [^{3}H]Ro 15-4513 and increasing concentrations of SH53d-acid. The concentrations resulting in half maximal inhibition of radioligand binding were converted into Ki values by using the Cheng-Prusoff relationship and the respective K$_D$ values given in Table 4.

Figure 6 Panel B shows the comparison of the KI values obtained from the B-Loop mutant α5P197T and α3T215P compared to wild-type receptors (Panel A). As can be seen, the compound SH53d-acid still binds to α5-mutant receptors at very high (nM) and to α3-mutant receptors at μM concentrations. It seems that Proline 197 in the B-loop of the benzodiazepine binding pocket does not contribute to the α5 selective binding properties of SH53d-acid.

Affinity change induced by conversion mutations confirm loop C as dominant molecular determinant of the selectivity

Figure 6 Panel C shows the Ki values obtained from the C-Loop mutants α3S257T and α5T239S. Exchanging the amino acid sequence from a threonine to a serine at position α5 239 / α3 257 in the C-loop of the subunits changed the binding properties of SH53d-acid in gaining nM binding to the α3-mutant while shifting α5-mutant binding into the μM range. It can therefore be concluded that threonine 239 in the C-Loop of the benzodiazepine binding pocket contributes heavily to the α5-selective binding properties of SH53d-acid. (For detailed statistical analysis see Supplemental Figure 2). For the parent compound SH53d-ester the influence of threonine 239 in the C-Loop is much less pronounced (see Supplemental Figure 2).

In line with the Ki values, we also observe a right shifted dose response in the modulation of α5T239S (EC50 of 555nM versus 60 nM in the WT), and no change in EC50 for the B-loop mutant, see Figure 6. Both mutants do not impact strongly on efficacy.

Figure 6

Discussion

Subtype selective ligands of the benzodiazepine binding site of $GABA_A$ receptors are highly desirable both as research tools to study the role of individual receptor subtypes in neuronal circuits and CNS function (Drexler et al., 2013; Sieghart, 2015), and to selectively modulate these receptors in experiments investigating animal models of diseases, as well as GABA effects in non-neuronal cells that express $GABA_A$ receptors. Due to the high homology of the six α subunits, and particularly of the four diazepam sensitive α1, 2, 3, 5 subunits, compounds with pronounced selectivity are still very rare (Rudolph and Mohler, 2014). One of the first α5β3γ2-selective compounds reported was L-655,708 (Quirk et al., 1996), a benzodiazepine negative allosteric modulator, which exerts its subtype selectivity via high affinity binding, while showing no change in efficacy (Casula et al., 2001). The imidazobenzodiazepine SH-053-2′F-R-CH3 (SH53d-ester) proved to be the first α5β3γ2-selective positive allosteric modulator (Savic et al., 2010). Here, we present the pharmacology of a derivative of the α5-preferring compound SH53d-ester with improved $GABA_A$ α5-subunit selective properties. This novel compound SH53d-acid displays a 40-fold higher affinity towards α5-containing receptors. In addition, it shows pronounced efficacy selectivity: The maximal modulation of GABA EC_{3-5} achieved at high concentrations is 3-fold higher in α5β3γ2 compared to α1β3γ2. This combination of affinity and efficacy – selectivity enables a specific concentration range (up to ~30 nM) where other α-containing receptors are not yet modulated, while GABA currents in α5-receptors are markedly enhanced.

SH53d-acid has already been shown to be effective as an airway smooth muscle relaxant (Forkuo et al., 2017). Airway smooth muscle cells contain several $GABA_A$ receptor subunits, where among the α subunits, only α4 and α5 are expressed (Mizuta et al., 2008; Gallos et al., 2015; Yocum et al., 2015). It has been demonstrated previously that targeting $GABA_A$ receptors containing either one of these subunits leads to relaxation of pre-contracted *ex vivo*

19

ASM from guinea pig, mouse and human (Gallos et al., 2015; Yocum et al., 2015), and indeed so does SH53d-acid (Forkuo et al., 2017).

A combination of computational modelling, mutagenesis and radioligand binding assays has been used in order to determine the amino acids responsible for the exceptional α5-subtype selectivity of SH53d-acid. The benzodiazepine ligand binding site is situated at the extracellular interface between adjacent α and γ subunits and is being lined by amino acids located in seven so-called "loops". Loops A, B and C are on the principal (+) side of the α-, while loops D, E, F and G are on the complementary (-) side of the γ2-subunit (Richter et al., 2012; Middendorp et al., 2014). The amino acids of loop B (GSYAY**T** in the subunits α1, α2 and α3; GSYAY**P** in α4, α5 and α6) have been studied previously in order to understand how they are involved in ligand binding. Especially α1-alanine 160 seems to contribute to the benzodiazepine binding site, while α1-threonine 162 seemed to be of less importance (Morlock and Czajkowski, 2011). In our experiments, this region in loop B did not contribute to the α5 selective binding properties of SH53d-acid. Our findings are in line with Moody et al (Moody and Jenkins, 2018), who describe that mutations in loop B made no significant shifts in affinity and only modest changes in maximum whole cell current modulation to benzodiazepine (such as midazolam) binding.

Loop C, on the other hand, has long been known to be important for ligand binding, since it is more variable than the other loops (Michalowski et al., 2017). α1-serine 206 (neighboring the serine mutated in our study) seems to interact physically with diazepam (Luscher et al., 2012). Both α1-serine 206 as well as α1-tyrosine 209 are important in determining the binding affinities for ligands of the benzodiazepine binding (Buhr et al., 1997) and S206 has been shown to influence the efficacy of midazolam to modulate GABA induced currents (Moody and Jenkins, 2018) as well as the affinities for β-carboline binding (Derry et al., 2004). The neighboring amino acid α1-threonine 207 specifically alters benzodiazepine affinity, while leaving binding unaffected (Morlock and Czajkowski, 2011).

In our study mutating the conserved Serine **S**xTGEY in the subunits α1, α2, α3, α4 and α6 versus **T**STGEY in α5 had a huge influence in shifting binding affinities, proving to be the

20

dominant molecular determinant of drug selectivity. While the S>T mutation is conserved, the threonine sidechain has an additional methyl group, and thus a larger volume and hydrophobic surface. It could be speculated that ligand burial is improved, leading to a more efficient change in conformation and higher affinity of binding.

Two recently released cryo-EM structures feature binding modes of flumazenil and alprazolam that are otherwise quite different, but they share the positioning of the imidazole-ring, which bears the acid group. Computational docking of the SH53d-acid results on both predictions, i.e. the compound can assume a flumazenil- like or an alprazolam-like position in the pocket. In both cases the acid group in the vicinity of loop C. Thus, our docking results correlate well with experimental evidence, but do not differentiate between these two known binding modes. The cryo-EM structures were obtained with human subunits, while our experimental data was obtained with rat subunits. The α isoforms are highly conserved across mammalian species (%ID between rat and human subunits is 98% for α1 and α3, and 96% for α5, respectively. The binding sites are 100% conserved) and both rodent and human subunits are broadly used to characterize benzodiazepines. Thus, the use of the human structural data is valid for the interpretation of our experimental data.

In the current study we provide the detailed pharmacological characterization of SH53d-acid and describe its superior (>40-fold) affinity selectivity for α5-containing GABA$_A$ receptors. This makes SH53d-acid a potentially very useful research tool for applications such as slice electrophysiology, due to its much wider window of selectivity. In addition, in the current study we were able to identify the molecular basis for drug selectivity: Computational docking combined with mutational analysis identified loop C of the GABA$_A$ receptor α-subunit as the dominant molecular determinant of drug selectivity. Thus, we characterize a promising novel α5-subunit-selective drug candidate and suggest that this atom level structural hypothesis can now be utilized towards a structure guided design of further novel compounds with similarly pronounced selectivity and otherwise improved properties. As suggested based on in vivo data from murine asthma models (Forkuo et al., 2017), this compound might be suitable for clinical development as a topical asthma

medication. Compared to the –ester or –amide analogues, it is more selective, and as an acid, is expected to be very inefficient in passing the blood brain barrier.

Additionally, our results may pave the way to improved α5-subunit-selective drug candidates useful also for CNS applications based on screening compounds into pharmacophore models based on the SH53d-acid bound state model. There is still big interest in α5-subunit-selective CNS permeant positive modulators, for example to alleviate certain symptoms of schizophrenia (Gill and Grace, 2014; Jacob, 2019).

Acknowledgements

23

Author contributions

Participated in research design: Ernst, Scholze

Conducted experiments: Simeone, Koniuszewski, Müllegger, Smetka, Steudle, Puthenkalam

Performed data analysis: Simeone, Steudle, Scholze, Koniuszewski, Ernst

Wrote or contributed to the writing of the manuscript: Ernst, Simeone, Koniuszewski and

Scholze

References

Barragan A, Weidner JM, Jin Z, Korpi ER and Birnir B (2015) GABAergic signalling in the immune system. *Acta Physiol (Oxf)* **213**(4): 819-827.

Belelli D and Lambert JJ (2005) Neurosteroids: endogenous regulators of the GABA(A) receptor. *Nat Rev Neurosci* **6**(7): 565-575.

Brickley SG and Mody I (2012) Extrasynaptic GABA(A) receptors: their function in the CNS and implications for disease. *Neuron* **73**(1): 23-34.

Buhr A, Schaerer MT, Baur R and Sigel E (1997) Residues at positions 206 and 209 of the α1 subunit of GABAA receptors influence affinities for benzodiazepine binding site ligands. *Mol Pharmacol* **52**(4): 676-682.

Casula MA, Bromidge FA, Pillai GV, Wingrove PB, Martin K, Maubach K, Seabrook GR, Whiting PJ and Hadingham KL (2001) Identification of amino acid residues responsible for the α5 subunit binding selectivity of L-655,708, a benzodiazepine binding site ligand at the GABA(A) receptor. *J Neurochem* **77**(2): 445-451.

Chen C and Okayama H (1987) High-efficiency transformation of mammalian cells by plasmid DNA. *MolCell Biol* **7**(8): 2745-2752.

Cheng Y and Prusoff WH (1973) Relationship between the inhibition constant (K1) and the concentration of inhibitor which causes 50 per cent inhibition (I50) of an enzymatic reaction. *Biochem Pharmacol* **22**(23): 3099-3108.

Derry JM, Dunn SM and Davies M (2004) Identification of a residue in the GABAA receptor α subunit that differentially affects diazepam-sensitive and -insensitive benzodiazepine site binding. *J Neurochem* **88**(6): 1431-1438.

Drexler B, Zinser S, Huang S, Poe MM, Rudolph U, Cook JM and Antkowiak B (2013) Enhancing the function of α5-subunit-containing GABAA receptors promotes action potential firing of neocortical neurons during up-states. *Eur J Pharmacol* **703**(1-3): 18-24.

Elgarf AA, Siebert DCB, Steudle F, Draxler A, Li G, Huang S, Cook JM, Ernst M and Scholze P (2018) Different Benzodiazepines Bind with Distinct Binding Modes to GABAA Receptors. *ACS Chem Biol* **13**(8): 2033-2039.

Fischer BD, Licata SC, Edwankar RV, Wang ZJ, Huang S, He X, Yu J, Zhou H, Johnson EM, Jr., Cook JM, Furtmuller R, Ramerstorfer J, Sieghart W, Roth BL, Majumder S and Rowlett JK (2010) Anxiolytic-like effects of 8-acetylene imidazobenzodiazepines in a rhesus monkey conflict procedure. *Neuropharmacol* **59**(7-8): 612-618.

Fleck MW, Thomson JL and Hough LB (2012) Histamine-gated ion channels in mammals? *Biochem Pharmacol* **83**(9): 1127-1135.

Forkuo GS, Nieman AN, Kodali R, Zahn NM, Li G, Rashid Roni MS, Stephen MR, Harris TW, Jahan R, Guthrie ML, Yu OB, Fisher JL, Yocum GT, Emala CW, Steeber DA, Stafford DC, Cook JM and Arnold LA (2018) A Novel Orally Available Asthma Drug Candidate That Reduces Smooth Muscle Constriction and Inflammation by Targeting GABAA Receptors in the Lung. *Mol Pharm* **15**(5): 1766-1777.

Forkuo GS, Nieman AN, Yuan NY, Kodali R, Yu OB, Zahn NM, Jahan R, Li G, Stephen MR, Guthrie ML, Poe MM, Hartzler BD, Harris TW, Yocum GT, Emala CW, Steeber DA, Stafford DC, Cook JM and Arnold LA (2017) Alleviation of Multiple Asthmatic Pathologic Features with Orally Available and Subtype Selective GABAA Receptor Modulators. *Mol Pharm* **14**(6): 2088-2098.

Gallos G, Yocum GT, Siviski ME, Yim PD, Fu XW, Poe MM, Cook JM, Harrison N, Perez-Zoghbi J and Emala CW, Sr. (2015) Selective targeting of the α5-subunit of GABAA receptors relaxes airway smooth muscle and inhibits cellular calcium handling. *Am J Physiol Lung Cell Mol Physiol* **308**(9): L931-942.

Gill KM and Grace AA (2014) The role of α5 GABAA receptor agonists in the treatment of cognitive deficits in schizophrenia. *Curr Pharm Des* **20**(31): 5069-5076.

Gladkevich A, Korf J, Hakobyan VP and Melkonyan KV (2006) The peripheral GABAergic system as a target in endocrine disorders. *Auton Neurosci* **124**(1-2): 1-8.

Hanrahan JR, Chebib M and Johnston GA (2011) Flavonoid modulation of GABA(A) receptors. *Br J Pharmacol* **163**(2): 234-245.

Hoerbelt P, Lindsley TA and Fleck MW (2015) Dopamine directly modulates GABAA receptors. *J Neurosci* **35**(8): 3525-3536.

Jacob TC (2019) Neurobiology and Therapeutic Potential of α5-GABA Type A Receptors. *Front Mol Neurosci* **12**: 179.

Jones G, Willett P, Glen RC, Leach AR and Taylor R (1997) Development and validation of a genetic algorithm for flexible docking. *J Mol Biol* **267**(3): 727-748.

Khom S, Strommer B, Ramharter J, Schwarz T, Schwarzer C, Erker T, Ecker GF, Mulzer J and Hering S (2010) Valerenic acid derivatives as novel subunit-selective GABAA receptor ligands - in vitro and in vivo characterization. *Br J Pharmacol* **161**(1): 65-78.

Liu S, Xu L, Guan F, Liu YT, Cui Y, Zhang Q, Zheng X, Bi GQ, Zhou ZH, Zhang X and Ye S (2018) Cryo-EM structure of the human α5β3 GABAA receptor. *Cell Res* **28**(9): 958-961.

Lorenz M, Kabir MS and Cook JM (2010) A two step synthesis of BzR/GABAergic active flavones via a Wacker-related oxidation. *Tetrahedron Lett* **51**(7): 1095.

Luscher BP, Baur R, Goeldner M and Sigel E (2012) Influence of GABA(A) receptor α subunit isoforms on the benzodiazepine binding site. *PloS one* **7**(7): e42101.

Masiulis S, Desai R, Uchański T, Serna Martin I, Laverty D, Karia D, Malinauskas T, Zivanov J, Pardon E, Kotecha A, Steyaert J, Miller KW and Aricescu AR (2019) GABAA receptor signalling mechanisms revealed by structural pharmacology. *Nature* **565**(7740): 454-459.

Michalowski MA, Kraszewski S and Mozrzymas JW (2017) Binding site opening by loop C shift and chloride ion-pore interaction in the GABAA receptor model. *Phys Chem Chem Phys* **19**(21): 13664-13678.

Middendorp SJ, Puthenkalam R, Baur R, Ernst M and Sigel E (2014) Accelerated discovery of novel benzodiazepine ligands by experiment-guided virtual screening. *ACS Chem Biol* **9**(8): 1854-1859.

27

Mizuta K, Xu D, Pan Y, Comas G, Sonett JR, Zhang Y, Panettieri RA, Jr., Yang J and Emala CW, Sr. (2008) GABAA receptors are expressed and facilitate relaxation in airway smooth muscle. *Am J Physiol Lung Cell Mol Physiol* **294**(6): L1206-1216.

Mohler H (2011) The rise of a new GABA pharmacology. *Neuropharmacol* **60**(7-8): 1042-1049.

Moody OA and Jenkins A (2018) The role of loops B and C in determining the potentiation of GABAA receptors by midazolam. *Pharmacol Res Perspect* **6**(6): e00433.

Morlock EV and Czajkowski C (2011) Different residues in the GABAA receptor benzodiazepine binding pocket mediate benzodiazepine efficacy and binding. *Mol Pharmacol* **80**(1): 14-22.

Olsen RW and Sieghart W (2008) International Union of Pharmacology. LXX. Subtypes of GABA(A) receptors: classification on the basis of subunit composition, pharmacology, and function. Update. *Pharmacol Rev* **60**(3): 243-260.

Phulera S, Zhu H, Yu J, Claxton DP, Yoder N, Yoshioka C and Gouaux E (2018) Cryo-EM structure of the benzodiazepine-sensitive α1β1γ2S tri-heteromeric GABAA receptor in complex with GABA. *Elife* **7**.

Quirk K, Blurton P, Fletcher S, Leeson P, Tang F, Mellilo D, Ragan CI and McKernan RM (1996) [3H]L-655,708, a novel ligand selective for the benzodiazepine site of GABAA receptors which contain the α5 subunit. *Neuropharmacol* **35**(9-10): 1331-1335.

Richter L, de Graaf C, Sieghart W, Varagic Z, Morzinger M, de Esch IJ, Ecker GF and Ernst M (2012) Diazepam-bound GABAA receptor models identify new benzodiazepine binding-site ligands. *Nat Chem Biol* **8**(5): 455-464.

Rudolph U and Mohler H (2014) GABAA receptor subtypes: Therapeutic potential in Down syndrome, affective disorders, schizophrenia, and autism. *Annu Rev Pharmacol Toxicol* **54**: 483-507.

Sali A and Blundell TL (1993) Comparative protein modelling by satisfaction of spatial restraints. *J Mol Biol* **234**(3): 779-815.

Saras A, Gisselmann G, Vogt-Eisele AK, Erlkamp KS, Kletke O, Pusch H and Hatt H (2008)
Histamine action on vertebrate GABAA receptors: direct channel gating and
potentiation of GABA responses. *J Biol Chem* **283**(16): 10470-10475.

Savic MM, Majumder S, Huang S, Edwankar RV, Furtmuller R, Joksimovic S, Clayton T, Sr.,
Ramerstorfer J, Milinkovic MM, Roth BL, Sieghart W and Cook JM (2010) Novel
positive allosteric modulators of GABAA receptors: do subtle differences in activity at
α1 plus α5 versus α2 plus α3 subunits account for dissimilarities in behavioral effects
in rats? *Prog Neuropsychopharmacol Biol Psychiatry* **34**(2): 376-386.

Sengupta S, Weeraratne SD, Sun H, Phallen J, Rallapalli SK, Teider N, Kosaras B, Amani V,
Pierre-Francois J, Tang Y, Nguyen B, Yu F, Schubert S, Balansay B, Mathios D,
Lechpammer M, Archer TC, Tran P, Reimer RJ, Cook JM, Lim M, Jensen FE,
Pomeroy SL and Cho YJ (2014) α5-GABAA receptors negatively regulate MYC-
amplified medulloblastoma growth. *Acta Neuropathol* **127**(4): 593-603.

Siebert DCB, Bampali K, Puthenkalam R, Varagic Z, Sarto-Jackson I, Scholze P, Sieghart
W, Mihovilovic M, Schnürch M and Ernst M (2018) Engineered benzodiazepine
binding site reveals functional conservation of allosteric GABAA receptor binding
sites. *ACS Chem Biol* **13**(8): 2040-2047.

Sieghart W (2015) Allosteric Modulation of GABAA Receptors via Multiple Drug-Binding
Sites. *Adv Pharmacol* **72**: 53-96.

Sieghart W and Savic MM (2018) International Union of Basic and Clinical Pharmacology.
CVI: GABAA Receptor Subtype- and Function-selective Ligands: Key Issues in
Translation to Humans. *Pharmacol Rev* **70**(4): 836-878.

Sigel E, Baur R, Racz I, Marazzi J, Smart TG, Zimmer A and Gertsch J (2011) The major
central endocannabinoid directly acts at GABA(A) receptors. *PNAS* **108**(44): 18150-
18155.

Sigel E and Luscher BP (2011) A closer look at the high affinity benzodiazepine binding site
on GABAA receptors. *Curr Top Med Chem* **11**(2): 241-246.

Simeone X, Siebert DCB, Bampali K, Varagic Z, Treven M, Rehman S, Pyszkowski J, Holzinger R, Steudle F, Scholze P, Mihovilovic MD, Schnurch M and Ernst M (2017) Molecular tools for GABAA receptors: High affinity ligands for β1-containing subtypes. *Sci Rep* **7**(1): 5674.

Stamenic TT, Poe MM, Rehman S, Santrac A, Divovic B, Scholze P, Ernst M, Cook JM and Savic MM (2016) Ester to amide substitution improves selectivity, efficacy and kinetic behavior of a benzodiazepine positive modulator of GABAA receptors containing the α5 subunit. *Eur J Pharmacol* **791**: 433-443.

Wan Y, Wang Q and Prud'homme GJ (2015) GABAergic system in the endocrine pancreas: a new target for diabetes treatment. *Diabetes Metab Syndr Obes* **8**: 79-87.

Yocum GT, Gallos G, Zhang Y, Jahan R, Stephen MR, Varagic Z, Puthenkalam R, Ernst M, Cook JM and Emala CW (2015) Targeting the GABA Receptor α4 Subunit in Airway Smooth Muscle to Alleviate Bronchoconstriction. *Am J Respir Cell Mol Biol*.

Zhu S, Noviello CM, Teng J, Walsh RM, Jr., Kim JJ and Hibbs RE (2018) Structure of a human synaptic GABAA receptor. *Nature* **559**(7712): 67-72.

Footnotes

Funding information:

This study was supported by the Austrian Science fund FWF, doctoral college W1232 "Molecular drug targets".

Figure Legends

Figure 1: Chemical structures of the two compounds.

Figure 2: Affinity and efficacy data in the four diazepam-sensitive GABA$_A$ receptor subtypes.

In order to directly compare the properties of SH53d-acid and SH53d-ester, both were measured at identical conditions side by side

A) and **B**): Inhibition of binding of [^{3}H]Flunitrazepam to recombinant αxβ3γ2 GABA$_A$ receptors. Membranes from HEK 293 cells transfected with the GABA$_A$ receptor subunit combinations were incubated with 2 nM [^{3}H]Flunitrazepam in the presence of various concentrations of SH53d-ester (Panel A) or SH53d-acid (Panel B). Values are given as mean ± SD, of three experiments performed in duplicates each.

C) and **D**): Concentration-response curves of the compounds SH53d-ester (Panel C) or SH53d-acid (Panel D) in αxβ3γ2 GABA$_A$ receptors expressed in *X. laevis* oocytes, using GABA EC$_{3-5}$. Values are given as mean ± SD, n=3 or higher from at least two batches of oocytes.

Figure 3: The benzodiazepine pocket of the Cryo-EM structure (6D6T) and the human α5 subunit in 6A96.

Color coding: Amino-acids differing between α5 and α1 are marked in cyan. γ2 subunit is light-grey. α5 and α1 subunits in pale yellow. **A)** The benzodiazepine pocket of the α1 (pale yellow) / γ2(grey) GABA$_A$ receptor with the pocket forming amino acids in stick rendering. B) The principal subunit of the benzodiazepine pocket of the α5 subunit. **C)** Partial alignment of the α1 and α5 subunits, with the mutated amino acids marked by cyan boxes, pocket forming amino acids from the γ2 subunit. For comparison with the rat amino acid numbering see Supplemental Table 2.

Figure 4: Comparison of alprazolam and flumazenil binding modes with representative results from the top 20 SH53d-acid poses:

(A) 6HUO with alprazolam; (B) representative alprazolam- like (BM II) pose; (C) 6D6T with flumazenil; (D) representative flumazenil-like (BMI) pose. Color coding: Pale yellow ribbons: α1/α5 subunits, grey ribbons: γ2 subunit; stick rendering: O red, N blue. The Ser/Thr position in which α5 sequence is uniquely featuring Thr is also shown in stick representation.

Figure 5: [³H]Flunitrazepam equilibrium binding assays.

Membranes from transfected HEK 293 cells were incubated with 1-20 nM (panels A and B) and 5-150 nM (panel C) [³H]Flunitrazepam in absence or presence of 5 µM diazepam (to determine non-specific binding). Radioactivity bound to the membranes were determined after rapid filtration. Inserts show the Scatchard Transformation of the results. Data represent a single experiment performed in duplicates each. Experiments were repeated 3-4 times with similar results.

Figure 6: inhibition constants (Ki) of SH53d-acid competition for [³H]Ro 15-4513 binding and TEV functional data in α5T239S-β3γ2 and α5P197T-β3γ2 injected oocytes

Panels A-C: Membranes from transfected HEK 293 cells were incubated with 5 nM [³H]Ro 15-4513 in the presence of various concentrations of SH53d-acid. The concentrations resulting in half maximal inhibition of radioligand binding were converted into Ki values by using the Cheng-Prusoff relationship and the respective K_D values given in Table 4. For detailed statistical analysis see Supplemental Figure 3. Panel C-D: Concentration-response curves and respective fitting parameters of SH53d-acid in mutated αxβ3γ2 GABA$_A$ receptors expressed in *X. laevis* oocytes. Values are given as mean ± SD, n=4-5 for at least two batches of oocytes.

Tables

<u>**Table 1:**</u> **Cloning Primers**

Primer sequences for the cloning of mutated α3- and α5- GABA$_A$ receptor subunits. Mutated bases are highlighted in bold. Numbering corresponds to precursor proteins based on the UniProtKB-accession IDs P20236 and P19969.

Q5-α3-T215P-FW	CTATGCCTAT**c**CCAAAGCTGAAG
Q5- α3-T215P-RV	CTTCCAAACTTCAGTGGAC
Q5-α3-S257T-FW	GATAATCCGG**a**CTAGTACAGG
Q5-α3-S257T-RV	TCTGTCCCAACAACATGAC
Q5-α5-197T-FW	TTATGCTTAC**a**CTAATTCGGAAG
Q5-α5-197T-RV	CTGCCAAATTTCAGGGGAC
Q5-α5-239S-FW	AACATCAGCA**g**CAGCACAGGT
Q5-α5-239S-RV	CTCAGTGCCTACTGTCTGC

Table 2: Potency of [³H]Flunitrazepam displacement in αxβ3γ2 receptors recombinantly expressed in HEK 293 cells.

The concentrations resulting in half maximal inhibition of specific binding from the experiment

shown in Figure 2A and 2B were converted to Ki values using the Cheng-Prusoff relationship

(see Methods). Data is reported as mean ± SD from three displacement curves performed in

duplicates each.

Compound	Ki ± SD in μM				α1/α5
	α1	α2	α3	α5	
SH53d-ester	1.9 ± 0.5	3.3 ± 0.6	1.6 ± 0.4	0.22 ± 0.03	9
SH53d-acid	1.6 ± 0.44	0.53 ± 0.14	0.65 ± 0.22	0.039 ± 0.003	**41**

Table 3: **Efficacy at αxβ3γ2 receptor expressed in *Xenopus laevis* oocytes given as %**

of control current at 30 nM concentration of the compound.

Subunit combinations expressed in *X. laevis* oocytes were analyzed as shown in Figure 1C

and 1D. The currents at 30 nM were intrapolated via non-linear regression analysis from the

curves shown. Respective EC50 values are given below.

| Compound	% of control current at 30 nM (EC50)				
	α1	α2	α3	α5	α1/α5
SH53d-ester	105 (5.0 µM)	108 (4.4 µM)	112 (1.6 µM)	138 (0.7 µM)	1.3
SH53d-acid	112 (1.3 µM)	127 (0.4 µM)	120 (2.4 µM)	380 (0.09 µM)	**3.3**

Table 4: **Equilibrium binding constant (K$_D$) for [^{3}H]Ro 15-4513 binding to the different receptor subtypes**

Membranes from HEK 293 cells transfected with the subunit combinations as indicated were incubated with various concentrations of [^{3}H]Ro 15-4513 in the absence or presence of either 50 µM Ro 15-1788 (to determine unspecific binding). Results were analyzed using the equation Y=Bmax*X/(K$_D$+X). K$_D$ values are presented as mean values ± SD from 3-5 independent experiments performed in duplicates.

subunit combination	α3(wt)β3γ2	α3(T215P)β3γ2	α3(S257T)β3γ2
K$_D$ ± SD (nM)	10.45 ± 4.5	2.85 ± 1.12	13.57 ± 0.73

subunit combination	α5(wt)β3γ2	α5(P197T)β3γ2	α5(T239S)β3γ2
K$_D$ ± SD (nM)	0.16 ± 0.09	0.23 ± 0.04	0.47 ± 0.13

SH53d-acid

SH53d-ester

Fig 1

A

% 3H-Flunitrazepam

- α1β3γ2
- α2β3γ2
- α3β3γ2
- α5β3γ2

[SH53d-ester]

B

% 3H-Flunitrazepam

- α1β3γ2
- α2β3γ2
- α3β3γ2
- α5β3γ2

[SH53d-acid]

C

% of control current at EC3-5

- α1β3γ2
- α2β3γ2
- α3β3γ2
- α5β3γ2

[SH53d-ester]

D

% of control current at EC3-5

- α1β3γ2
- α2β3γ2
- α3β3γ2
- α5β3γ2

[SH53d-acid]

Fig 2

C
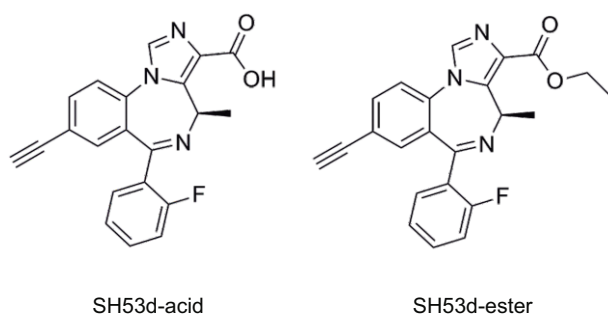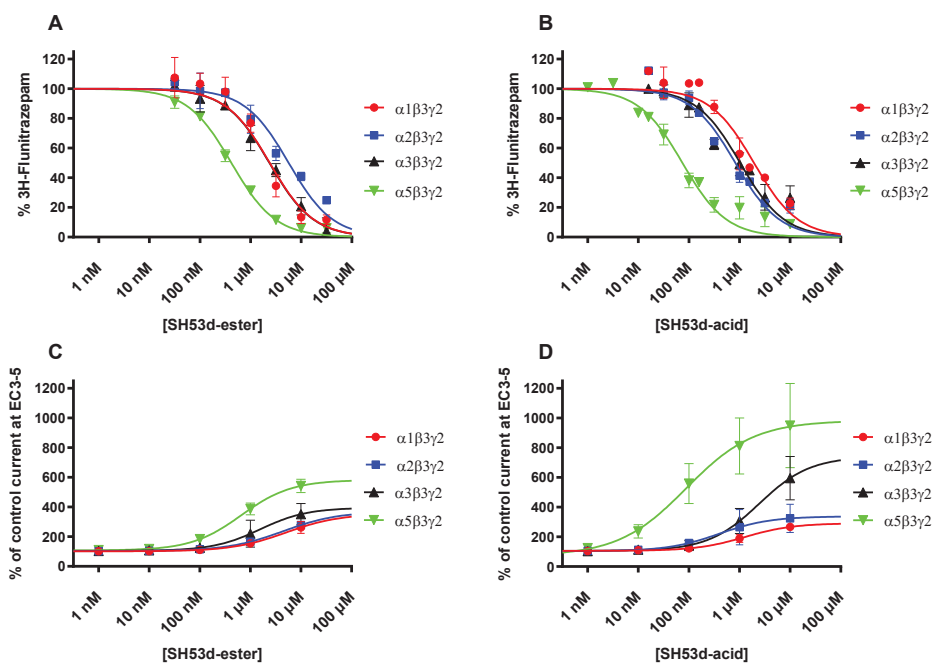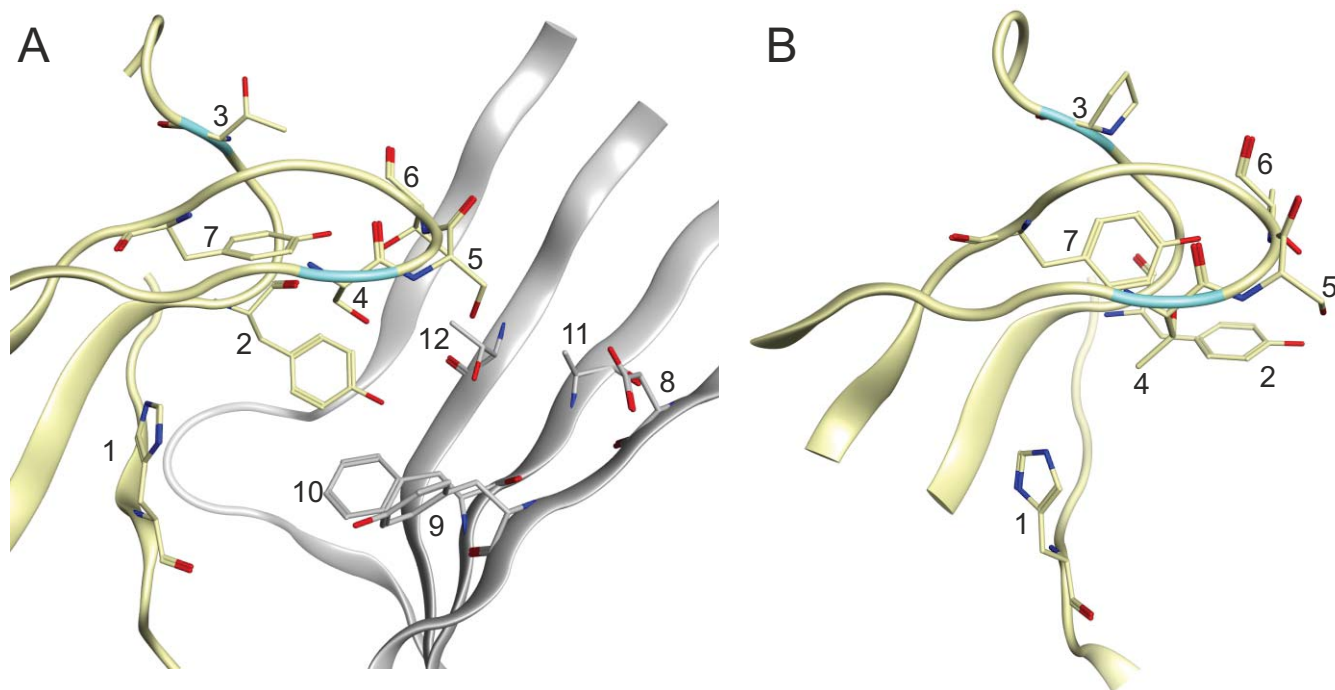
	Loop A		Loop B				Loop C				
Nr in picture	**1**		**2**		**3**			**4**	**5**	**6**	**7**
	102		160		163			205	206	207	210
alpha-1	F H N		Y A Y		T			Q	S S T G E		Y
	105		163		166			208	209	210	213
alpha-5	F H N		Y A Y		P			S	T S T G E		Y
					r197			r239			

	Loop G		Loop D		Loop E `	
Nr in picture	**8**	**9**	**10**	**11**	**12**	
	56	58	77	79	142	
gamma-2	T D M Y		F F A E		Y T L	

Fig 3

A 6HUO

α1   E   γ2

E'

C   D

B   G

A   alprazolam

B α5-model

α5   E   γ2

E'

C   D

B   G

A   SH53d-acid
(BM II)

C 6D6T

α1   E   γ2

E'

C   D

B   G

A   flumazenil

D α5-model

α5   E   γ2

E'

C   D

B   G

A   SH53d-acid
(BM I)

Fig 4

A α5β3γ2

B α5(P197T)β3γ2

C α5(T239S)β3γ2

Fig 5

A wild-type receptors

B B-loop mutants

C C-loop mutants

D

E

	α5(wt)-β3γ2	α5T239S-β3γ2	α5P197T-β3γ2
Hillslope	0.8 ± 0.2	0.9 ± 0.1	0.9 ± 0.2
Top	856 ± 53	944 ± 18	1219 ± 49
EC50 (nM)	60 ± 22	555 ± 46	45 ± 11

Fig 6